IEEE Photonics Journal
An IEEE Photonics Society Publication

Open Access

Efficient Wavelength-Tunable Gain-Switching and Gain-Switched Mode-Locking Operation of a Heavily Er^{3+}-Doped ZBLAN Mid-Infrared Fiber Laser

Volume 9, Number 4, August 2017

Yanlong Shen
Yishan Wang
Kunpeng Luan
Hongwei Chen
Mengmeng Tao
Jinhai Si

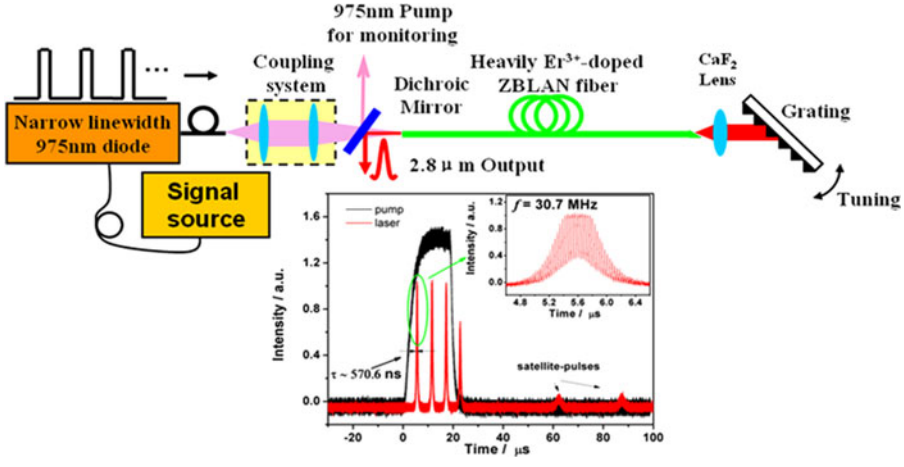

DOI: 10.1109/JPHOT.2017.2721998
1943-0655 © 2017 IEEE

IEEE photonics SOCIETY

IEEE

Efficient Wavelength-Tunable Gain-Switching and Gain-Switched Mode-Locking Operation of a Heavily Er^{3+}-Doped ZBLAN Mid-Infrared Fiber Laser

Yanlong Shen,[1,2,3,4,5] Yishan Wang,[1,5] Kunpeng Luan,[3] Hongwei Chen,[3] Mengmeng Tao,[3] and Jinhai Si[2]

[1]State Key Laboratory of Transient Optics and Photonics, Xi'an Institute of Optics and Precision Mechanics, Chinese Academy of Sciences, Xi'an 710119, China
[2]Shaanxi Key Laboratory of Photonics Technology for Information, School of Electronics and Information Engineering, Xi'an Jiaotong University, Xi'an 710049, China
[3]State Key Laboratory of Laser Interaction with Matter, Northwest Institute of Nuclear Technology, Xi'an 710024, China
[4]University of Chinese Academy of Sciences, Beijing 100049, China
[5]Collaborative Innovation Center of Extreme Optics, Shanxi University, Taiyuan 030006, China

DOI:10.1109/JPHOT.2017.2721998

Manuscript received April 22, 2017; revised June 20, 2017; accepted June 27, 2017. Date of publication July 3, 2017; date of current version July 19, 2017. This work was supported in part by the CAS/SAFEA International Partnership Program for Creative Research Teams and National Natural Science Foundation of China under Grants 11573058 and 61690222, and in part by the fund of the State Key Laboratory of Laser Interaction with Matter under Grant SKLLIM1503. Corresponding authors: Yanlong Shen and Yishan Wang (e-mail: shenyl@stu.xjtu.edu.cn; yshwang@opt.ac.cn).

Abstract: We report on an efficient wavelength-tunable gain-switched and gain-switched mode-locked Er^{3+}-doped double-clad fiber laser with a linear cavity. Stable gain-switching and gain-switched mode-locking were achieved with slope efficiencies of 28.6% and 34.5% with respect to launched pump power, respectively. The gain-switched laser pulses were generated with a maximum average output power of around 110 mW, pulse width of 661.2 ns, and calculated peak power of ~16.5 W at a repetition rate of 10 kHz. At the same repetition, the gain-switched mode-locked laser pulses were generated with a maximum average output power of around 514 mW, subpulse repetition rate of ~30.7 MHz, and peak power of higher than 154 W at a repetition rate of 10 kHz when the wavelength was tuned to 2.78 μm. This is, to the best of our knowledge, the first demonstration of a gain-switched self-started mode-locked fiber laser near 3 μm.

Index Terms: Lasers, fiber, pulsed, infrared and far-infrared lasers, tunable.

1. Introduction

Recently, rare-earth ions doped fluoride fiber lasers emitting at mid-infrared (Mid-IR) waveband have attracted much attention due to their potential applications in medicine, spectroscopy, and IR-laser pumping [1], [2]. Thus, lots of effort has been contributed to the development of mid-infrared ZBLAN fiber lasers [3]–[9]. Thanks to the coincidence of the wavelength (975 nm) of commercially available high power laser diode (LD) and the absorption band of the Erbium ion, the output power of LD

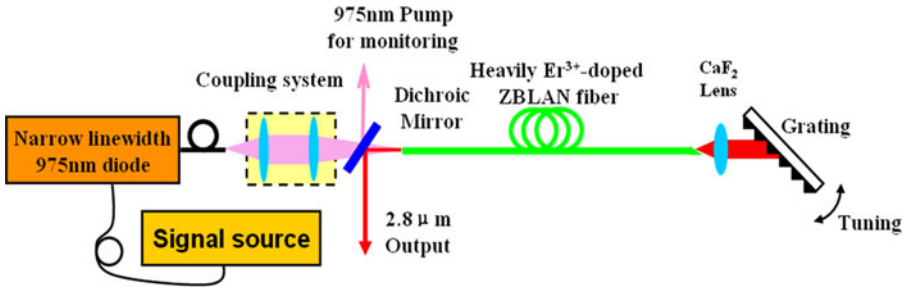

Fig. 1. Experimental setup of the tunable gain-switched mode-locked Er^{3+}-doped ZBLAN fiber laser.

pumped continuous wave (CW) Er^{3+}-doped ZBLAN fiber lasers have been scaled up significantly in the past decades, of which the published maximum power was claimed as high as 30 W [10].

However, pulsed laser is prior to the CW mode for many applications owing to its advantages of high precision, high sensitivity, and high response speed. Generally, two principal approaches, i.e., the Q-switching and mode-locking are employed to generate mid-infrared laser pulses [11]–[18]. A number of actively or passively Q-switched pulsed mid-infrared fiber lasers were demonstrated over the past years [11]–[14], and fiber laser pulse with a peak power of 37 kW was obtained at 2.9 μm in the mode-locking regime very recently, which enjoys the highest peak power in Mid-IR fiber laser pulses [18]. Nevertheless, there probably exist some disadvantages when these techniques were used in fluoride fiber lasers [19]. For one thing, absorbers or Q-switches are needed to insert into laser cavity, which increases complexity of cavity. For another, the inserted elements could lead to cavity losses, and reduce efficiency of the laser output. Aside from Q-switching and mode-locking, directly pumped by a pulsed laser, gain-switching could be an excellent candidate for producing pulsed output owing to the well-controlled pump pulse width, repetition rate and its convenience for amplification, which has been widely studied in Tm^{3+}-doped silica fiber lasers [20]–[22]. Gain-switched Er^{3+}-doped ZBLAN fiber laser is, therefore, supposed to offer a rather simple way to produce 2.8-μm laser pulses [23]. In 2001, Dickinson *et al.* reported a gain-switched Er^{3+}/Pr^{3+}-codoped ZBLAN 2.7 μm fiber laser, pumped by a pulsed Ti:sapphire laser, with a pulse energy of 1.9 mJ and pulse width of 18 μs [19]. In 2011, Gorjan *et al.* demonstrated a gain-switched Er^{3+}-doped ZBLAN fiber laser with an average power of 2 W, pulse width of 300 ns and corresponding peak power of 68 W at a repetition rate of 100 kHz [24].

In this work, we report on a diode-pumped, efficient, wavelength-tunable gain-switched and gain-switched mode-locked mid-infrared fiber laser by exploiting the $^4I_{11/2}$ to $^4I_{13/2}$ transition of erbium, emitting at 2.8 μm. Stable gain-switching was achieved with the repetition rate ranging from 1 to 10 kHz. Gain-switched mode-locking was attained with a sub-pulse repetition rate of $\sim$30.7 MHz by further increasing the pump pulse energy. The central wavelength of the pulsed laser was tunable from 2.71 to 2.83 μm by tuning the blazed grating in Littrow configuration.

2. Experimental Setup

The experimental setup for the tunable gain-switched mode-locked Er^{3+}-doped ZBLAN fiber laser is shown in Fig. 1. A narrow linewidth 975-nm fiber-coupled laser diode (LD), modulated by a signal source with a repetition rate (RR) range of 1 $\sim$ 10 kHz, was used as a pulsed pump source. The central wavelength of the LD is stabilized at 975.5 nm and the linewidth is kept around 0.7 nm. The pigtail fiber of the laser diode has a core diameter of 105 μm and a numerical aperture (NA) of 0.22, respectively. A piece of 3.1 m heavily (concentration of 6 mol%) Er^{3+}-doped ZBLAN multimode core double-clad fiber was adopted as the active fiber (fabricated by FiberLabs, Inc.). The other detailed parameters, including core, cladding, concentration, can be found in our previous work [14]. Both ends of the fiber were held by fiber chuck holders with a U-shaped groove heat sink. The pumping end of the fiber was carefully and perpendicularly cleaved to serve as the laser output port with

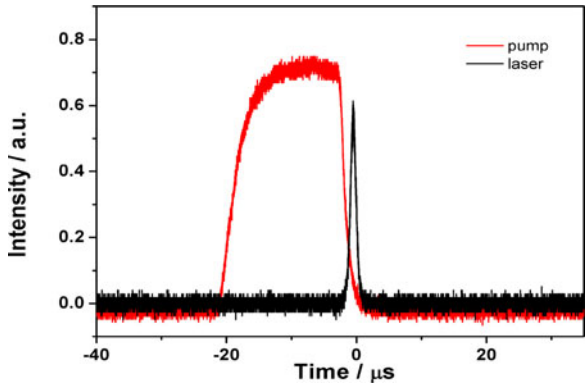

Fig. 2. Measured temporal characteristics of pump and laser pulse with 54.8 μJ pump at 10 kHz (10 μs/div).

a coupling ratio of 96% (Fresnel reflection $\sim$4%), while the other end was cleaved at an angle of about 10° to avoid the parasitic oscillating. The 975-nm LD pump light was coupled into the inner cladding of the active fiber through a compact coupling system comprised of a collimator and an aspheric lens with a coupling efficiency of $\sim$80%. A CaF_2 lens (L1) with a focal length of 15 mm was used to collimate the emission at 2.8 μm and steer it onto a gold-coated blaze grating, which was placed in the Littrow configuration to provide feedback and make the laser wavelength-tunable. The parameters of the grating are grooves of 625 mm^{-1}, blaze wavelength of 2.8 μm and blaze angle of 61.2°. The total length of the laser cavity was about 3.2 m. A dichroic mirror (high reflection $>$99.5% at 2.8 μm, high transmission $>$95% at 975 nm) was placed with an incidence angle of 45° between the pumping end and coupling system to couple out the laser beam for measuring. The measuring devices included a thermal powermeter (Gentec, XLP12-3S-H2-D0) for measuring the laser power, a HgCdTe detector (Vigo PVM-2TE-10.6, rise time of less than 3 ns) and a 1 GHz digital oscilloscope for detecting and monitoring the waveforms respectively, and an optical spectrum analyzer (Andor Shamrock 750) with a resolution of as high as 0.2 nm for recording the laser spectrum.

3. Results and Discussion

3.1 Gain-Switching Operation

Firstly, we adjusted the grating to maximize the output power of the fiber laser under a certain CW pump above the threshold of $\sim$0.4 W. Thereafter, the LD pump was modulated by a signal source with a RR of 1 to 10 kHz and a duty-cycle of 20% to set the fiber laser at gain-switching operation. Variation of the pump pulse energy was realized by adjusting the pump power and the RR of the pump pulse. The gain-switched 2.8 μm fiber laser was easily achieved at a moderate pump energy. The laser and the pump diode pulses were measured simultaneously, as typically shown in Fig. 2 for the launched pump pulse energy of 54.8 μJ at a RR of 10 kHz. As can be seen in Fig. 2, during one pump period, only one laser pulse was generated. The laser performance in gain-switching operation with only one laser pulse during a pump period, i.e., without laser pulse spikes, was investigated at different pump pulse energies from 0 to 70 μJ. The minimum pulse width without pulse spikes was around 661.2 ns, and pulse spikes occurred when the pump energy was higher than 70 μJ.

The laser system can also work at lower RRs by tuning the RR of the pump pulses. In our experiment, the minimum and maximum pump RRs were 1 kHz and 10 kHz, respectively. Stable gain-switched pulse trains at both the minimum and maximum RRs were attained, as shown in Fig. 3. It can be seen that the laser pulse frequency is equal to the pump RR. The amplitude fluctuation of pulse trains (RMS, root mean square) was measured to be less than 5%. The stability could be improved on by using a highly stable LD source.

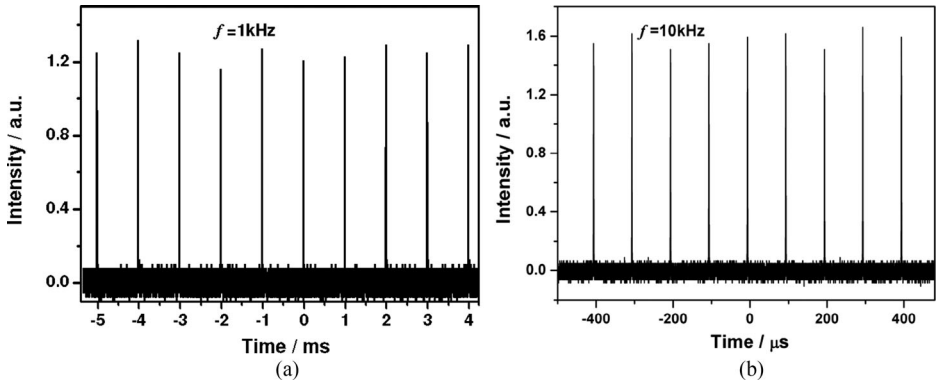

Fig. 3. Measured typical pulse trains of the minimum and maximum RRs in the experiment. (a) 2.8 μm pulse train at 1 kHz (1 ms/div). (b) 2.8 μm pulse train at 10 kHz (100 μs/div).

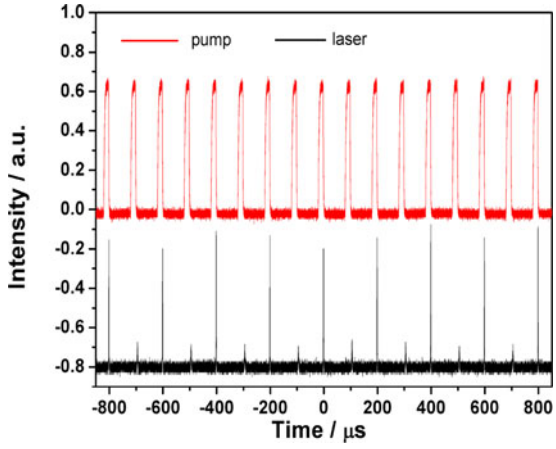

Fig. 4. Measured pulse train with a laser pulse frequency of 5 kHz in the experiment under a pump energy of ~49.7 μJ at a RR of 10 kHz (200 μs/div).

It should be pointed out, however, that the laser pulse frequency was not always the same as the RR of the pump source when the pump energy was lower than a particular value, for instance, 49.7 μJ at 10 kHz, as shown in Fig. 4. It can be seen that the laser pulse frequency was a half of the pump RR. That is, one pump pulse was not sufficient to obtain population inversion for laser oscillating between the laser transition levels of $^4I_{11/2}$ and $^4I_{13/2}$.

Presented in Fig. 5 are the measured FWHM (full width at half maximum) pulse width and calculated peak power at gain-switching mode as a function of launched pump power. As similar to the results in [21], the pulse width was inversely proportional to pump energy. The minimum pulse width without pulse spikes was around 661.2 ns, which was larger than that in [24] due to longer cavity length in our case. The output pulse width could be shortened by employing a shorter length gain fiber [22]. The peak power increased, as a whole, almost linearly with the pump energy although there was a break around the launched pump energy of ~50 μJ, and this was because the laser pulse frequency was a half of the pump RR when the launched pump energy was lower than 49.7 μJ. Combining the minimum pulse width and maximum pulse energy yielded the calculated maximum peak power of ~16.5 W in gain-switching mode without laser pulse spikes. Compared to our previous work with a feedback of a protected gold mirror (case A) [23], in which the maximum output peak power was barely 3.5 W, the output laser pulse in this case (case B) had much narrower pulse width and higher peak power. This significant enhancement of peak power could be explained via spectrum dynamics theory of pulsed pump erbium-doped fluoride fiber laser

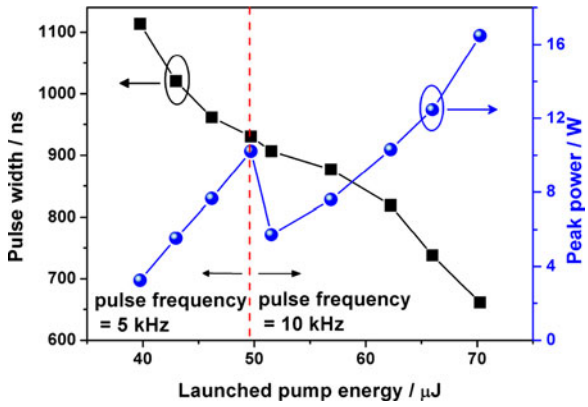

Fig. 5. Measured pulse width and calculated peak power at gain-switching mode varies with launched pump energy at the pump RR of 10 kHz.

[25], which shows that the spectrum evolution is time dependent. In other words, different temporal parts of the laser pulse possess different wavelengths. In case A, at the beginning of laser emission, the lower multiplet of level $^4I_{13/2}$ was empty and the laser oscillated at shorter wavelength. As soon as the lower multiplet was populated during laser emission, reabsorption losses built up at the short-wavelength side of the fluorescence band and the laser was forced to oscillate at a longer wavelength [19]. Both the spectrum and pulse width were, therefore, broadened simultaneously. When replacing the mirror with a wavelength selective element, for instance, a grating, the oscillating wavelength was locked and the linewidth was greatly narrowed under the same pump level.

3.2 Gain-Switched Mode-Locking Operation

If the pump energy was increased beyond 70 μJ in our experiment, the population of the upper laser level $^4I_{11/2}$ depleted along with a pulse output and then, the upper laser level repopulated during the remained pumping and depleted again. Consequently, a second pulse appeared, that is, pulse spikes occurred. The essence of the appearance of pulse spikes was regarded as the releasing of energy which was remained in the upper or lower laser level (particles in lower laser level could shift to the upper laser lever through the energy transfer upconversion process between the lower laser level particles, i.e., ETU2 process) after delivering the first pulse. When the pump energy was further increased to around 90 μJ, the gain-switched mode-locking was observed. A typical temporal profile of the laser pulse at gain-switched mode-locking state is shown in Fig. 6. The temporal separation between adjacent sub-pulses in an envelope was about 32.6 ns, consistent with the round-trip time of the 3.2 m linear laser cavity. This corresponded to a RR of 30.7 MHz which was the fundamental cavity frequency of the laser cavity. We attributed this self-started mode-locking in our gain-switched mode-locked fiber laser to the active fiber itself, which also played a role of a saturable absorber due to the excited state absorption (ESA) from the long life-time $^4I_{13/2}$ level ($\sim$9 ms) [26]. The possible mechanism about the transition between the gain-switching and gain-switched mode-locking could result from the saturable absorber effect introduced by the reabsorption. And the process could be interpreted as follows on the whole. At the lower pump level, the gain in the cavity was switched by the depletion of the particles in the upper laser level. As increasing the pump power, the particles in the lower laser level accumulated more and more, which played two roles in the laser pulse oscillation. On one hand, the particles in the lower level shifted to the upper level through ETU2 process, and then participated in the amplification of the laser pulse. On the other hand, the particles in the lower level reabsorbed the laser signal. And thus, the gain was switched by the particles in both the upper and lower laser levels. The detailed physical origin of this self-started gain-switched mode-locking is still under investigation through numerical simulation.

As increasing the pump power, energy absorbed by the ions became more and more. And thus, there was still residual energy stored in the excited states even though the pump stopped.

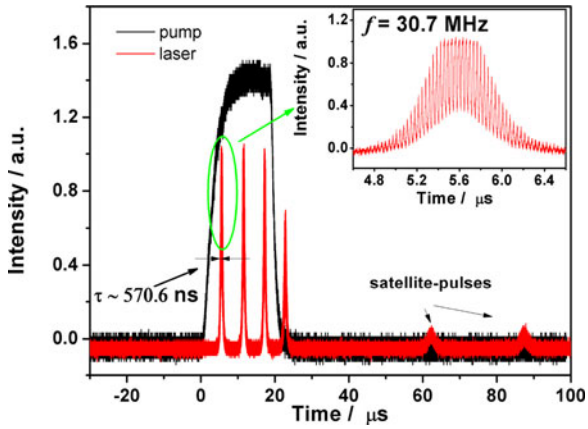

Fig. 6. Measured gain-switched mode-locking pulse with a laser pulse energy of 51.4 μJ (maximum output energy) under a 183.7 μJ pump at the pump RR of 10 kHz. Inset: the details of a single envelope over 160 ns duration.

Therefore, following the main gain-switched envelopes with a time interval of ~40 μs, there were some satellite-pulses, which indicated that the energy was still stored in the $^4I_{13/2}$ level and the upper laser $^4I_{11/2}$ level repopulated through energy transfer upconversion between particles in $^4I_{13/2}$ level (ETU2 process) and depleted again, releasing satellite-pulses [27].

As shown in Fig. 6, the total laser pulse energy during a pump period was 51.4 μJ and the energy of the first gain-switched envelope was estimated to be higher than 12.9 μJ, assuming the total energy distributed uniformly in each envelope. Considering the FWHM width of the first envelope (570.6 ns), the peak power of the gain-switched envelope was calculated to be 19.9 W (assuming the pulse in a Sech^2 shape), which was slightly higher than the peak power at gain-switched operation. The peak power of mode-locked pulse was estimated by the equation [27]:

$$P_{pk} = (E_{gs}/\Delta\tau_{gs})/(\Delta\tau_{ml}/T) \tag{1}$$

where E_{gs} and $\Delta\tau_{gs}$ are the energy and the FWHM of the gain-switched envelope, respectively. $\Delta\tau_{ml}$ is the measured individual pulse width and T is the period of mode-locked pulses in the gain-switched envelope. The width of the individual pulses cannot be resolved directly since it is below the resolution of the photodetector. The temporal measurements in our experiment suggest an average value of 4.8 ns, however, the exact pulse width is believed to be much shorter. However we could use it to estimate the minimum peak power of the gain-switched mode-locked pulses. Substituting values obtained above into Eq. (1) gave the peak power of mode-locked pulse of at least 154 W.

The laser average output power at the pump RR of 10 kHz is plotted in Fig. 7. The average power increased linearly with launched pump power with slop efficiencies of 28.6% and 34.5% at gain-switching mode and gain-switched mode-locking mode, respectively. The slope efficiency of gain-switched mode-locking was very close to the result in [24], which also reached the Stokes limit of ~35% (the ratio of the pump wavelength to the laser wavelength). However, in such a highly Er^{3+}-doped (6 mol%) fiber, the calculated results showed that the theoretical efficiency could excess Stokes limit and reach ~50% due to the energy-recycling regime, and the efficiency increased with increasing the pump power [28]. The theoretical slope efficiency of this fiber laser can be expressed by the equation below [8]:

$$\eta = \eta_s \eta_m \eta_L \eta_E = \eta_s \eta_m \frac{\ln(1-T)}{\ln[(1-T)(1-L)]}\left[2 - \frac{b_1^2 W_{22}}{b_2^2 W_{11}}\right] \tag{2}$$

where

η is the laser slope efficiency,

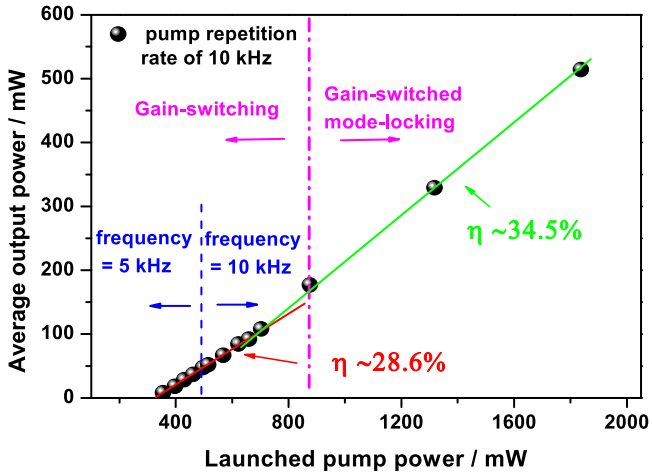

Fig. 7. Average output power as a function of launched pump power at the pump RR of 10 kHz.

η_S is the Stokes limit (~35%),
η_m is the geometrical overlap of the pump and signal modes,
η_L is the cavity loss efficiency reduction factor,
η_E is the efficiency enhancement factor resulting from pump energy-recycling regime,
T is the cavity output coupling ratio,
L the round-trip intra-cavity loss,
W_{11} and W_{22} are the ETU parameters of the lower and upper laser level, respectively.
b_1 and b_2 are the Boltzmann occupation factors of the lower and upper laser levels.

In our case, the cavity output coupling ratio is around 4% provided by Fresnel reflection at the fiber facet-air interface. The roundtrip cavity loss was estimated to be 2.87 dB. The Boltzmann occupation factors b_1 and b_2 are 0.113 and 0.2, respectively, and W_{11} and W_{22} were calculated to be 3.84 and 1.24, which were deduced from the data of [28]. Take the above values into consideration, we calculated the η_L of 0.75, and η_E of 1.9. If the fiber is pumped with core pumping, the η_m could be roughly unity. Thus, the theoretical slop efficiency could reach 49.8%. In practice, the geometrical overlap of the pump and signal modes is lower than unity, and the reabsorption which could introduce the saturable absorber effect for mode-locking could also decrease the overall efficiency, consequently, the experimental result of slop efficiency was commonly much lower than the calculated value.

There was also an increase in the laser slope efficiency when increasing the pump power in [10], in which they attributed the change to the wavelength shift of the pump diodes when their driving current is increased. However, the wavelength of the LD in our case kept stable due to the locking effect of the grating inside the LD. The difference in slope efficiency between the gain-switching mode and gain-switched mode-locking mode could be explained as follows. At gain-switching operation under lower pump powers, particles in the long-life-time state $^4I_{13/2}$ level through the transition from the upper $^4I_{11/2}$ level were not crowded enough to exploit the process of ETU2. As a result, the slope efficiency was much lower than the Stokes efficiency. Increasing the pump power to make the laser operate at gain-switched mode-locking can improve the population of $^4I_{13/2}$ level, and subsequently the role of ETU2 appeared more important. Therefore, the higher the pump power was, the more the particles in $^4I_{13/2}$ level, and thus the more impact of the energy recycling scheme on the enhancement of the slope efficiency [28]. The linearity of the curve and no saturation observed in our system verified that the average output power could be further scaled up by simply increasing the pump power.

Laser spectra at gain-switching and gain-switched mode-locking operation modes were recorded by an optical spectrum analyzer with a resolution of 0.2 nm, as typically shown in Fig. 8. The central wavelengths were stabilized at 2777.3 nm with a FHWM linewidth of about 1.5 nm at both

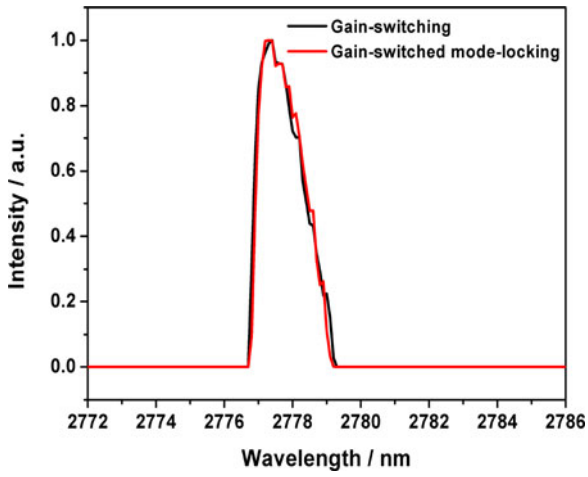

Fig. 8. Typical spectra of the laser output at the gain-switching (black line) and gain-switched mode-locking modes (red line).

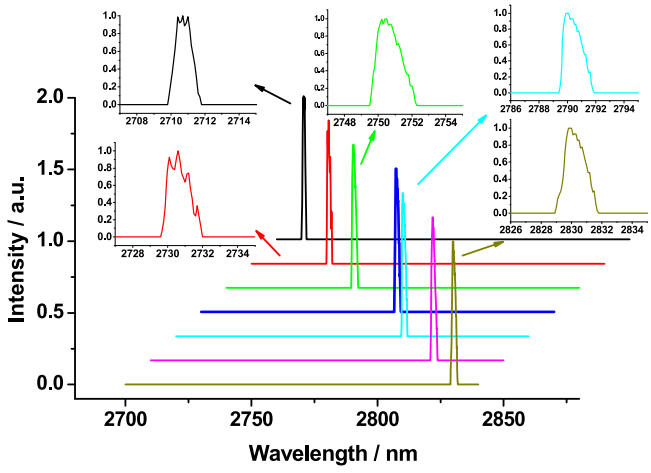

Fig. 9. Typical output spectra of the laser output at gain-switched mode-locking modes at 10 kHz when tuning the grating.

gain-switching and gain-switched mode-locking modes. Generally, mode-locking state is featured with a broadened optical spectrum. However, with a grating in the laser cavity, the center wavelength and the bandwidth were essentially unchanged during the experiment due to the wavelength-locking effect of the grating feedback [29].

The tunable output spectra in gain-switched mode-locking operation are typically shown in Fig. 9. The FHWM linewidths of the laser pulses were kept around 1.5 nm during the entire tuning range. It can be seen that there are some ripples in the top of the spectra when the operating wavelengths were shorter than 2750 nm, and the ripple almost disappeared as tuning the wavelengths to longer than 2770 nm. It is thought that the atmospheric water vapor absorption lines might lead to the ripples because the vapor absorption below 2750 nm is much stronger [18].

Fixing the RR of the pump source at 10 kHz, the output power at different wavelength is shown in Fig. 10 under the maximum launched pump power of 1.8 W in our experiment. The laser average power in gain-switched mode-locked regime was higher than 200 mW in the waveband of 2710∼2830 nm. The output power was maximized at 2777.3 nm and decreased in both sides, which matched well with the intra-cavity gain profile in [1]. Compared with the tuning curves in the CW regime, the tuning range in [5] was slightly narrower than in [7]. Under the same pump level of around 5 W, the tuning range in [7] was 2700–2840 nm, while the tuning range in our case was 2710–2830 nm (under the pump power of ∼2 W, the parameters of our fiber close to [7]).

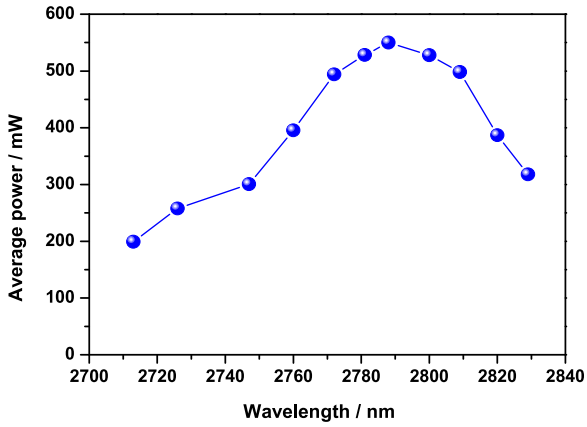

Fig. 10. Measured average output power as a function of wavelength at 10 kHz under the maximum launched pump power of 1.8 W.

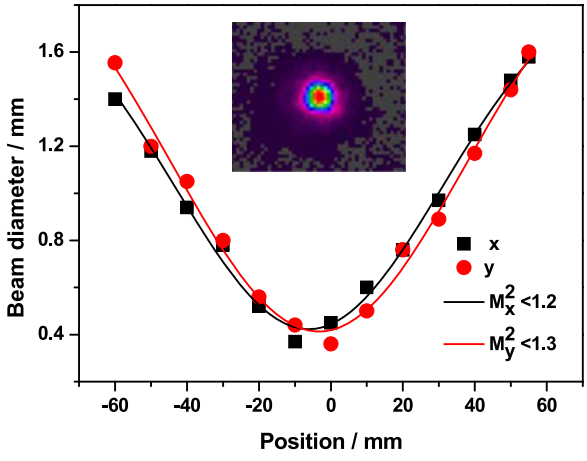

Fig. 11. Laser beam diameters as a function of distance from the waist location (where $z = 0$). Inset: Far-field image of the laser beam.

The caustic measurements was performed to measure the laser beam quality factor M^2 [30], and the results of these measurements are shown in Fig. 11. The far-field beam spot had a symmetrical Gaussian distribution, and the beam quality M^2 was calculated to be less than 1.2 and 1.3 for x-axis and y-axis, respectively.

4. Conclusion

In conclusion, we have demonstrated a tunable gain-switched and gain-switched mode-locked Er^{3+}-doped ZBLAN fiber laser operating at 2.8 μm. Gain-switched self-started mode-locking with an average power of 514 mW was attained with a sub-pulse repetition rate of ~30.7 MHz at a repetition rate of 10 kHz. The wavelength of pulsed output was tunable over a 100-nm wavelength ranging from 2.71 to 2.83 μm through tuning the grating. The laser could be used as a seed source for master oscillator power amplifier (MOPA) at mid-infrared region.

Acknowledgment

The authors are very grateful to Biao Sun from Precision Measurements Group (Singapore Institute of Manufacturing Technology) and Xiaohong Hu from State Key Laboratory of Transient Optics and Photonics (Xi'an Institute of Optics and Precision Mechanics, Chinese Academy of Sciences) for fruitful discussions.

References

[1] S. D. Jackson, "Towards high-power mid-infrared emission from a fibre laser," *Nature Photon.*, vol. 6, no. 7, pp. 423–431, 2012.

[2] X. S. Zhu and N. Peyghambarian, "High-power ZBLAN glass fiber lasers: Review and prospect," *Adv. OptoElectron.*, vol. 2010, pp. 1–23, 2010.

[3] B. Srinivasan, J. Tafoya, and R. Jain, "High-power "Watt-level" CW operation of diode-pumped 2.7 μm fiber lasers using efficient cross-relaxation and energy transfer mechanisms," *Opt. Exp.*, vol. 4, no. 12, pp. 490–495, 1999.

[4] S. D. Jackson, T. A. King, and M. Pollnau, "Diode-pumped 1.7-W erbium 3-μm fiber laser," *Opt. Lett.*, vol. 24, no. 16, pp. 1133–1135, 1999.

[5] X. Zhu and R. Jain, "Compact 2 W wavelength-tunable Er: ZBLAN mid-infrared fiber laser," *Opt. Lett.*, vol. 32, no. 16, pp. 2381–2383, 2007.

[6] X. Zhu and R. Jain, "10-W-level diode-pumped compact 2.78 μm ZBLAN fiber laser," *Opt. Lett.*, vol. 32, no. 1, pp. 26–28, 2007.

[7] S. Tokita, M. Hirokane, M. Murakami, S. Shimizu, M. Hashida, and S. Sakabe, "Stable 10 W Er:ZBLAN fiber laser operating at 2.71–2.88 μm," *Opt. Lett.*, vol. 35, no. 23, pp. 3943–3945, 2010.

[8] D. Faucher, M. Bernier, G. Androz, N. Carnon, and R. Vallée, "20 W passively cooled single-mode all-fiber laser at 2.8 μm," *Opt. Lett.*, vol. 36, no. 7, pp. 1104–1106, 2011.

[9] S. Tokita, M. Murakami, S. Shimizu, M. Hashida, and S. Sakabe, "Liquid-cooled 24 W mid-infrared Er:ZBLAN fiber laser," *Opt. Lett.*, vol. 34, no. 20, pp. 3062–3064, 2009.

[10] V. Fortin, M. Bernier, S. T. Bah, and R. Vallée, "30 W fluoride glass all-fiber laser at 2.94 μm," *Opt. Lett.*, vol. 40, no. 12, pp. 2882–2885, 2015.

[11] T. Hu, D. D. Hudson, and S. D. Jackson, "Actively Q-switched 2.9 m Ho^{3+}/Pr^{3+}-doped fluoride fiber laser," *Opt. Lett.*, vol. 37, no. 11, pp. 2145–2147, 2012.

[12] S. Tokita, M. Murakami, S. Shimizu, M. Hashida, and S. Sakabe, "12 W Q-switched Er:ZBLAN fiber laser at 2.8 μm," *Opt. Lett.*, vol. 36, no. 15, pp. 2812–2814, 2011.

[13] C. Wei, X. Zhu, R. A. Norwood, and N. Peyghambarian, "Passively Q-switched 2.8 μm nanosecond fiber laser," *IEEE Photon. Technol. Lett.*, vol. 24, no. 19, pp. 1741–1744, Oct. 2012.

[14] Y. Shen *et al.*, "Watt-level passively Q-switched heavily Er^{3+}-doped ZBLAN fiber laser with a semiconductor saturable absorber mirror," *Sci. Rep.* vol. 6, 2016, Art. no. 26659.

[15] J. Li, D. D. Hudson, Y. Liu, and S. D. Jackson, "Efficient 2.87 μm fiber laser passively switched using a semiconductor saturable absorber mirror," *Opt. Lett.*, vol. 37, no. 18, pp. 3747–3749, 2012.

[16] S. Duval, M. Bernier, V. Fortin, J. Genest, M. Piché, and R. Vallée, "Femtosecond fiber lasers reach the mid-infrared," *Optica*, vol. 2, no. 7, pp. 623–626, 2015.

[17] P. Tang *et al.*, "Watt-level passively mode-locked Er–doped ZBLAN fiber laser at 2.8 μm," *Opt. Lett.*, vol. 40, no. 21, pp. 4855–4858, 2015.

[18] S. Antipov, D. D. Hudson, A. Fuerbach, and S. D. Jackson, "High-power mid-infrared femtosecond fiber laser in the water vapor transmission window," *Optica*, vol. 3, no. 12, pp. 1373–1376, 2016.

[19] B. Dickinson, P. Golding, M. Pollnau, T. A. King, and S. D. Jackson, "Investigation of a 791-nm pulsed-pumped 2.7-μm Er-doped ZBLAN fiber laser," *Opt. Commun.*, vol. 191, no. 3, pp. 315–321, 2001.

[20] Y. Tang, L. Xu, Y. Yang, and J. Xu, "High-power gain-switched Tm^{3+}-doped fiber laser," *Opt. Exp.*, vol. 18, no. 22, pp. 22964–22972, 2010.

[21] N. Simakov, A. Hemming, S. Bennetts, and J. Haub, "Efficient, polarised, gain-switched operation of a Tm-doped fibre laser," *Opt. Exp.*, vol. 19, no. 16, pp. 14949–14954, 2011.

[22] M. Jiang and P. Tayebati, "Stable 10 ns, kilowatt peak-power pulse generation from a gain-switched Tm-doped fiber laser," *Opt. Lett.*, vol. 32, no. 13, pp. 1797–1799, 2007.

[23] Y. Shen *et al.*, "Gain-switched 2.8 μm Er^{3+}-doped double-clad ZBLAN fiber laser," *Proc. SPIE*, vol. 9453, pp. 9453E-1–9453E-6, 2015.

[24] M. Gorjan, R. Petkovšek, M. Marinček, and M. Čopič, "High-power pulsed diode-pumped Er:ZBLAN fiber laser," *Opt. Lett.*, vol. 36, no. 10, pp. 1923–1925, May 2011.

[25] M. Gorjan, M. Marincek, and M. Čopič, "Spectral dynamics of pulsed diode-pumped erbium-doped fluoride fiber lasers," *J. Opt. Soc. Amer. B*, vol. 27, no. 12, pp. 2784–2793, 2010.

[26] P. S. Golding, S. D. Jackson, T. A. King, and M. Pollnau, "Energy transfer processes in Er^{3+}-doped and Er^{3+},Pr^{3+}-codoped ZBLAN glasses," *Phys. Rev. B*, vol. 62, no. 2, pp. 856–864, 2000.

[27] H. Tsao, C. Chang, S. Lin, J. Sheu, and T. Tsai, "Passively gain-switched and self mode-locked thulium fiber laser at 1950 nm," *Opt. Laser Technol.*, vol. 56, pp. 354–357, 2014.

[28] M. Pollnau and S. D. Jackson, "Energy recycling versus lifetime quenching in erbium-doped 3 μm fiber lasers," *IEEE J. Quantum Electron.*, vol. 38, no. 2, pp. 162–169, Feb. 2002.

[29] F. Wang, D. Shen, D. Fan, and Q Lu, "Spectrum narrowing of high power Tm: Fiber laser using a volume bragg grating," *Opt. Exp.*, vol. 18, no. 9, pp. 8937–8941, 2010.

[30] D. Flamm *et al.*, "Fast M^2 measurement for fiber beams based on modal analysis," *Appl. Opt.*, vol. 51, no. 87, pp. 987–993, 2012.